Brain Advance Access published July 29, 2016

BRAIN
A JOURNAL OF NEUROLOGY

Auto-antibodies to contactin-associated protein 1 (Caspr) in two patients with painful inflammatory neuropathy

Kathrin Doppler,[1] Luise Appeltshauser,[1] Carmen Villmann,[2] Corinna Martin,[2,3] Elior Peles,[4] Heidrun H. Krämer,[5] Axel Haarmann,[1] Mathias Buttmann[1] and Claudia Sommer[1]

Auto-antibodies against the paranodal proteins neurofascin-155 and contactin-1 have recently been described in patients with chronic inflammatory demyelinating polyradiculoneuropathy and are associated with a distinct clinical phenotype and response to treatment. Contactin-associated protein 1 (Caspr, encoded by *CNTNAP1*) is a paranodal protein that is attached to neurofascin-155 and contactin-1 (CNTN1) but has not yet been identified as a sole antigen in patients with inflammatory neuropathies. In the present study, we screened a cohort of 35 patients with chronic inflammatory demyelinating polyradiculoneuropathy (age range 20–80, 10 female, 25 male) and 22 patients with Guillain-Barré syndrome (age range 17–86, eight female, 14 male) for auto-antibodies against paranodal antigens. We identified two patients, one with chronic inflammatory demyelinating polyradiculo-neuropathy and one with Guillain-Barré syndrome, with autoantibodies against Caspr by binding assays using Caspr transfected human embryonic kidney cells and murine teased fibres. IgG3 was the predominant autoantibody subclass in the patient with Guillain-Barré syndrome, IgG4 was predominant in the patient with chronic inflammatory demyelinating polyradiculoneuropathy. Accordingly, complement deposition after binding to HEK293 cells was detectable in the patient with IgG3 autoantibodies only, not in the patient with IgG4. Severe disruption of the paranodal and nodal architecture was detectable in teased fibres of the sural nerve biopsy and in dermal myelinated fibres, supporting the notion of the paranodes being the site of pathology. Deposition of IgG at the paranodes was detected in teased fibre preparations of the sural nerve, further supporting the pathogenicity of anti-Caspr autoantibodies. Pain was one of the predominant findings in both patients, possibly reflected by binding of patients' IgG to TRPV1 immunoreactive dorsal root ganglia neurons. Our results demonstrate that the paranodal protein Caspr constitutes a new antigen that leads to autoantibody generation as part of the novel entity of neuropathies associated with autoantibodies against paranodal proteins.

1 Department of Neurology, University of Würzburg, Germany
2 Institute for Clinical Neurobiology, University of Würzburg, Germany
3 Department of Anesthesiology, University of Würzburg, Germany
4 Department of Molecular Cell Biology, Weizmann Institute of Science, Rehovot, Israel
5 Department of Neurology, University of Gießen, Germany

Correspondence to: Dr. Kathrin Doppler,
Department of Neurology, University of Würzburg,
Josef-Schneider-Str. 11, 97080 Würzburg,
Germany
E-mail: Doppler_K@ukw.de

Keywords: Keywords: contactin-associated protein; autoantibodies; paranodopathy; CIDP; GBS

Abbreviations: Caspr = contactin-associated protein 1; CIDP = chronic inflammatory demyelinating polyradiculoneuropathy; DRG = dorsal root ganglia; GBS = Guillain-Barré syndrome; HEK = human embryonic kidney

Received March 21, 2016. Revised June 7, 2016. Accepted June 19, 2016.

Introduction

The nodes of Ranvier are essential for saltatory nerve conduction along myelinated nerve fibres and are divided into the nodal, paranodal and juxtaparanodal compartments, which consist of different adhesion proteins and ion channels (Dupree *et al.*, 1999). At the paranodes, the protein complex consisting of neurofascin-155, contactin-1 (encoded by *CNTN1*) and Caspr (encoded by *CNTNAP1*) forms a link between myelin sheath and axon (Susuki *et al.*, 2008). Recent studies have shown that this paranodal complex is a target for autoantibodies against the proteins contactin-1, neurofascin-155 and the contactin-1/Caspr complex in patients with chronic inflammatory demyelinating polyradiculoneuropathy (CIDP) (Devaux *et al.*, 2012; Ng *et al.*, 2012; Querol *et al.*, 2013; Doppler *et al.*, 2015*b*; Miura *et al.*, 2015). Antibodies against neurofascin-155 and contactin-1 are associated with a distinct clinical picture of severe acute-onset motor and sensory neuropathy, and often with tremor or ataxia (Querol *et al.*, 2014; Doppler *et al.*, 2015*b*; Miura *et al.*, 2015). Although neuropathies with these paranodal antibodies have only been detected in a small percentage of patients with inflammatory neuropathies, they are of diagnostic interest, as there is evidence that these patients may respond less well to the standard therapy of CIDP (Querol *et al.*, 2014, 2015; Doppler *et al.*, 2015*b*). So far, information on this rare condition is limited, as only a few patients have been identified and reported. In the present study, we prospectively screened serum from a cohort of patients with inflammatory neuropathies for binding to murine teased fibres and thereby identified the paranodal protein Caspr as a new antigen for autoantibodies against the paranodal complex.

Materials and methods

Patients

Patients with a diagnosis of CIDP fulfilling the Inflammatory Neuropathy Cause and Treatment (INCAT) criteria (Hughes *et al.*, 2008) or Guillain-Barré syndrome (GBS) according to the Brighton criteria (Sejvar *et al.*, 2011) who attended the University Hospitals Würzburg or Gießen between January 2014 and November 2015, were prospectively recruited. The resulting cohort comprised 35 patients with CIDP (age range 20–80, 10 female, 25 male) and 10 patients with GBS (age range 17–86, 8 female, 14 male). To increase the number of GBS samples, plasma exchange material of 12 patients with GBS that was stored in the Department of Neurology, University Hospital Würzburg, was retrospectively included. Healthy controls and disease controls (patients with multiple sclerosis or myasthenia gravis) for binding assays with Caspr-transfected human embryonic kidney (HEK) 293 cells and murine teased fibres were taken from serum samples recruited for a former study that were stored in our department (Doppler *et al.*, 2015*a*, *b*). The study and the use of sera from the previous study were approved by the Ethics Committees of the Medical Faculties of the Universities of Würzburg and Gießen, and all patients gave informed and written consent to participate.

Binding assays with murine teased fibres

Murine sciatic nerves and ventral and dorsal roots were obtained from adult C57BL/6 mice, and teased fibre preparations and binding assays with human sera and plasma exchange material were performed as previously described (Doppler *et al.*, 2015*a*, *b*). Briefly, teased fibre preparations were incubated with patients' sera diluted 1:100 overnight at 4°C following incubation with appropriate anti-human IgG Cy3-conjugated secondary antibodies (Dianova, 1:100) for 1 h at room temperature. Double immunofluorescence staining using polyclonal rabbit anti-Caspr (Abcam, 1:1000) and corresponding anti-rabbit IgG Cy3-conjugated and anti-human IgG Cy2-conjungated secondary antibodies (Jackson ImmunoResearch, 1:100) was performed to detect co-localization of sera and the paranodal complex. Slides were assessed using a fluorescence microscope (Zeiss Ax10, Zeiss).

ELISA for autoantibodies against contactin-1 and neurofascin-155

ELISA for anti-contactin-1 and anti-neurofascin-155 was performed as previously described (Ng *et al.*, 2012; Doppler *et al.*, 2015*a*). Briefly, Maxisorb 96-well-plates (Thermo Fisher Scientific) were coated with human full-length contactin-1 (Sino Biological) or neurofascin-155 (kindly provided by J. K. Ng and E. Meinl; Ng *et al.*, 2012). All wells were incubated with either patients' samples (1:100), anti-contactin-1 (mouse monoclonal, Abcam, 1:200) or anti-neurofascin antibodies (chicken polyclonal, R&D, 1:5000). Plates were then incubated with appropriate horseradish-peroxidase-conjugated secondary antibodies (anti-human-IgG for patients' material, 1:10 000, Dako; anti-mouse IgG/-chicken IgY for the control antibody, anti-mouse: Dako, 1:500, anti-chicken: Thermo Fisher Scientific, 1:10 000). TMB (tetramethylbenzidine) solution (eBioscience) was added to each well and the reaction was stopped after 15 min by the addition of 50 µl of 1 M sulphuric acid. Optical density was measured at 450 nm with a Multiskan EX Elisa Reader (Thermo Fisher Scientific). The normal value was set at 5 standard deviations (SD) above the mean of 60 healthy controls, based on the distribution of values obtained from normal controls and anti-contactin-1-positive/anti-neurofascin-positive CIDP patients from a former study (Doppler *et al.*, 2015*a*,*b*).

Binding assays with transfected HEK293 cells and flow cytometry

HEK293 cells were plated onto poly-D-lysine-coated cover slips in a 24-well-plate at a density of 50 000 cells/well and were transiently transfected with plasmids of human Caspr (Peles *et al.*, 1997) or human contactin-1 as a control (Peles *et al.*, 1995) using the calcium-phosphate precipitation method (0.25 µg of DNA/well) as previously described (Doppler *et al.*, 2015*a*, *b*). A transfection rate of about 20% was achieved.

Binding assays were performed 48 h after transfection by incubating the cells for 1 h with the serum samples of the two patients who showed paranodal binding to murine teased fibres (1:500) and then fixing them with 4% paraformaldehyde. The cells were then incubated with Cy3-conjugated anti-human IgG as a secondary antibody. Immunofluorescence staining with mouse monoclonal anti-contactin-1 (Abcam, 1:200) or anti-Caspr (UC Davis/NIH NeuroMab Facility, 1:200) with corresponding Cy3-conjungated anti-mouse IgG secondary antibodies was performed as a control. For the identification of IgG subclasses, FITC-conjugated anti-human IgG1, IgG2, and IgG4 (Abcam, 1:200) or anti-human IgG3 (Sigma Aldrich, 1:200) were used as secondary antibodies. Coverslips were mounted using Mowiol (Calbiochem) with DAPI. Immunostaining was assessed using a fluorescence microscope (Zeiss Ax10). The examiners (L.A., K.D.) were blinded to the diagnosis of the patients and controls. For flow cytometry, cells were co-transfected with plasmids of Caspr and contactin-1, as it is known that contactin-1 is required for cell surface expression of Caspr (Faivre-Sarrailh *et al.*, 2000). Cells were detached with Accutase® (GE Healthcare), rinsed, suspended in flow cytometry buffer containing 1% bovine serum albumin and subsequently incubated with sera of either patients or healthy controls (1:50) or a polyclonal rabbit anti-Caspr-antibody (Abcam, 1:50) as a positive control. After a washing step, the corresponding secondary Cy2-conjugated anti-human IgG or Alexa Fluor® 488-conjugated anti-rabbit IgG antibodies were added (Jackson ImmunoResearch, 1:50/Thermo Fisher Scientific, 1:50). Fluorescence data were acquired on a FACSCalibur™ flow cytometer using CellQuest software (BD Bioscience).

Pre-absorption experiments

Pre-absorption was performed by serial incubation of patients' samples (1:500 and 1:1000) 1 h each in three wells with Caspr-transfected HEK293 cells. Sera incubated in wells with contactin-1-transfected cells served as controls. Then, the samples were incubated with murine teased fibres, dorsal root ganglion (DRG) sections and cultured DRG neurons and labelled with anti-human IgG as described above.

Binding assays with cultured hippocampal neurons, motor neurons and dorsal root ganglia neurons

Hippocampi were dissected from C57BL/6 embryonic Day 18 mouse embryos, were transferred to pre-warmed trypsin-EDTA and were digested for 5 min. Neurobasal® medium was added and the hippocampi were triturated gently with a fire-polished Pasteur pipette. Cells were plated on poly-D-lysine coated cover slips at a density of 25 000 cells per plate and were grown for 7–14 days. Cells were fixed with 4% paraformaldehyde and were incubated with patients' samples (1:1000) and Cy3-conjugated anti-human IgG as a secondary antibody (Dianova, 1:100). For the dissection of DRG neurons, C57BL/6 wild-type mice aged 6–12 weeks were used. Animals were euthanized by CO_2 asphyxiation and cervical dislocation. DRG neurons were extracted from all parts of the spinal cord and treated with Liberase Blendzyme 4 (TH; 5U/500 µl, Sigma Aldrich) and Liberase™ Blendzyme 3 (1 U/100 µl, Sigma-Aldrich) as described (Dib-Hajj *et al.*, 2009). DRGs were kept and grown in 89% Dulbecco's modified Eagle medium/F12 high glucose. DRG neurons were plated at a density of 7×10^3 cells on glass cover slips coated with poly-L-lysine (20 µg/ml). Fixation and staining of the cells was performed 7 to 14 days after isolation. Mixed motor neuron cultures were prepared from spinal cord of embryonic Day 13 mouse embryos. Spinal cord pieces were digested with trypsin for 30 min at 37°C in a water bath. Trypsinization was stopped with foetal calf serum. Following trypsin digestion, the cell solution was supplied with Neurobasal® medium and triturated. The supernatant was supplied to a fresh tube and the cell debris again triturated. Both supernatants were combined and centrifuged for 20 min at 600 *g*. The cell pellet was resuspended in Neurobasal® medium containing L-glutamine and B27. Cells were counted and plated with a density of 300 000 cells /3 cm dish containing 4 polylysine-coated cover slips. Cells were grown for 4 weeks to reach full neuronal differentiation.

Binding assays with cerebellum, spinal cord, cortex and dorsal root ganglion sections

Cerebellum, spinal cord, cerebral cortex and DRG were prepared from adult Lewis rats and were cryoconserved. Cryosections were cut and incubated with patients' and control samples at a dilution of 1:100 and 1:500 each. Anti-human IgG (Dako) was used as a secondary antibody and was visualized with diaminobenzidine.

For double labelling of DRG, sections were incubated with patients' IgG and anti-TRPV1 (Alomone labs, 1:100) and biotin-conjugated IB4 (Sigma Aldrich, 1:500) as well as appropriate secondary antibodies (Alexa Fluor® 488-conjugated anti-human IgG, Dianova, 1:100, FITC-conjugated extravidin, Sigma, 1:200) and were assessed using a fluorescence microscope (Zeiss Ax10). Again, the examiner (K.D.) was blinded to the diagnosis.

Immunohistochemistry of skin biopsies and human teased fibres

Punch skin biopsies of the lateral index finger, proximal and distal leg of Patient 1 were taken as previously described (Doppler *et al.*, 2013). Double immunofluorescence with anti-MBP (GeneTex, 1:200), anti-Caspr (Abcam, 1:100), anti-pan-neurofascin (recognizing both isoforms, neurofascin-155 and -186, Abcam, 1:400) and anti-pan-sodium-channel (Sigma Aldrich, 1:100) was performed as previously described (Doppler *et al.*, 2013). Intraepidermal nerve fibre density was determined by immunofluorescence labelling with anti-PGP9.5 (Ultraclone, 1:1000) and counting of nerve fibres crossing the dermal-intraepidermal junction according to published counting rules (Lauria *et al.*, 2010). Sural nerve biopsy was performed according to standard procedures in Patient 1 (Dyck, 2005). One-quarter of the nerve biopsy was used for teased fibre preparations that were performed and immunolabelled according to the same protocol as used for murine teased fibres (Doppler *et al.*, 2015*a*, *b*). Double immunofluorescence staining was done with anti-MBP (GeneTex, 1:500) and anti-Caspr (Abcam, 1:100), anti-pan-neurofascin (Abcam,

1:400) and anti-pan-sodium-channel (Sigma Aldrich, 1:100). For the detection of binding of IgG at the paranodes, teased fibres were incubated with Cy3-conjugated anti-human IgG (Jackson ImmunoResearch, 1:100) or FITC-conjugated anti-human IgG1-4 antibodies (IgG1, 2 and 4: Abcam, IgG3: Sigma Aldrich; 1:200) for 1 h. All immunofluorescence stains were evaluated using a fluorescence microscope (Zeiss Axio).

Complement binding assay with C1q

Caspr-transfected HEK293 cells were washed with phosphate-buffered saline (PBS) and then incubated for 1 h at 37°C and constant agitation with patients' samples diluted 1:500 in 2% BSA/PBS. After three washing steps with PBS, human C1q (Sigma Aldrich, 200 µg/ml) was added and was incubated for 2 h at 37°C and constant agitation. After further washing and fixation with 4% PFA, FITC-conjugated anti-C1q (Abcam, 1:200) was used as a secondary antibody to detect deposition of C1q, performing double immunofluorescence with anti-human IgG Cy3-conjugated secondary antibody (Dianova, 1:200).

Results

Detection of autoantibodies against Caspr

Characteristic binding to the paranodes of murine teased fibres co-localizing with the immunofluorescence signal of anti-Caspr was observed in two patients, one with CIDP and one with GBS (Table 1 and Fig. 1A–I). No autoantibodies against neurofascin-155 or contactin-1 were detectable in these samples by ELISA. Both sera tested negative for autoantibodies against gangliosides GM1 IgM/IgG, GM2 IgM/IgG, GD1b IgM/IgG and GQ1b IgM/IgG (Euroimmun). Binding assays of the sera of both patients with Caspr-transfected HEK293 cells showed strong binding to transfected cells. No binding to Caspr-transfected HEK293 cells was found after incubation with the sera of 25 normal controls and 10 disease controls with other neurological autoimmune disorders. We did not detect any binding to cells transfected with contactin-1 (Fig. 2E and F). Binding of sera to Caspr-transfected HEK293 cells was assessed by fluorescence microscopy (Fig. 2A–F) and was further quantified by flow cytometry (Fig. 2G–I).

To confirm the specificity of the autoantibodies against Caspr, the samples of both patients were preincubated with Caspr and contactin-1 transfected HEK293 cells. Paranodal staining of teased fibres was lost after preincubation with Caspr, but not with contactin-1 (Fig. 1J–M), confirming the existence of autoantibodies specifically directed against Caspr in 1/35 patients with CIDP and 1/22 patients with GBS.

Using secondary antibodies directed against human IgG1–4, both in the teased fibres assay and the HEK293 cell assay, IgG4 was identified as the most prevalent subclass in Patient 1. No relevant immunoreactivity was found for IgG2 and IgG3 and only weak reactivity for IgG1. In Patient 2, IgG3 was the most prevalent subclass and no immunoreactivity of IgG1, IgG2 and IgG4 was detectable (Fig. 3 and Supplementary Fig. 1).

Clinical features of patients with anti-Caspr autoantibodies

Patient 1 was a 30-year-old male who developed sensory deficits and severe pain in the back and feet in January 2013, 2 weeks after a common cold. Pareses followed shortly after, symptoms were rapidly progressive, and the patient was unable to walk within a few months (Table 2). There were no autonomic symptoms. The patient suffered from severe neuropathic pain in the hands and feet that required treatment with high doses of tilidine and pregabalin (Table 2). CSF revealed a slightly increased cell count and high protein level (Table 2). Nerve conduction studies showed features of a demyelinating neuropathy including decreased nerve conduction velocity, prolonged distal motor latency and F waves and preserved compound muscle and sensory nerve action potentials at the onset of disease. No compound motor nerve action potentials were recordable 1 year after onset except for the right median nerve. EMG revealed fibrillations and positive sharp waves in distal more than in proximal muscles. An MRI scan of the lumbosacral plexus showed increased signal intensity in the spinal roots and the sciatic nerves of both sides. Symptoms were continuously progressive until the patient was mostly wheel-chair bound and was only able to walk a few steps with crutches. Treatment with intravenous immunoglobulins was ineffective. Methylprednisolone (1 g/day for 5 days) led to a slight improvement for only a few weeks. Plasma exchange was started in 2014 and resulted in stabilization of the patient's condition for several weeks. Treatment with rituximab was initiated in July 2014. The patient showed marked improvement after treatment with rituximab (2×1000 mg initially and 1×1000 mg after 6 months). Pareses as well as sensory deficits ameliorated over a period of 20 months. The patient was finally able to walk without aid. Furthermore, nerve conduction studies confirmed a partial recovery of the peripheral nerves. Binding to murine teased fibres had disappeared in an assay performed 5 months after the first treatment with rituximab. At this time, binding to transfected HEK293 cells was weak as confirmed by flow cytometry, and 6 months after treatment it was no more detectable (Supplementary Fig. 2).

Patient 2 was a 69-year-old female who developed pain in the back and legs and distal numbness followed by pareses of the hands and legs in 2011, 10 days after a respiratory infection. Pareses and sensory deficits increased over 3 weeks. There were no autonomic symptoms, but severe neuropathic pain in the arms and legs that was treated with up to 200 mg of pregabalin per day. Nerve conduction studies showed reduced compound muscle action potentials but normal nerve conduction velocities during the first week of disease. One week later, nerve conduction studies revealed prolonged F wave and distal motor latencies,

Table 1 Clinical data of anti-Caspr-positive patients

		Patient 1	Patient 2
Age at onset, gender		30 years, male	69 years, female
Diagnosis		CIDP	GBS
Symptoms		Pain of the back and feet, numbness of the lower arms and legs, tetraparesis (distal > proximal)	Pain of the feet and lower legs and back, tingling and numbness of the fingers, paresis of the hands and legs
Antecedent infection		Common cold 10 days prior to onset of disease	Respiratory infection 10 days prior to admission
Course of disease		Subacute to chronic, rapidly progressive with exacerbation during infections	Monophasic with a nadir of disease at 3 weeks.
Nerve conduction studies at onset	DML	Prolonged	Prolonged
	NCV	Reduced	Slightly reduced
	SNAP	Normal	Normal
	CMAP	Normal	Reduced
	CB	Yes, tibial nerve	Yes, tibial nerve
	Temporal dispersion	Yes	No
	F wave latency	Prolonged	Prolonged
	EMG spontaneous activity	Yes	No
	EMG during course of disease	Spontaneous activity	Normal
Nerve biopsy		Axonal degeneration, no features of demyelination	Not done
Treatment		IVIG ineffective, steroids temporarily effective, stabilization after PE, very good response to rituximab	5 PE, beginning recovery after 4 weeks, at 1 year completely recovered

CB = conduction block; CMAP = compound muscle action potential; DML = distal motor latency; IVIG = intravenous immunoglobulins; PE = plasma exchange; NCV = nerve conduction velocity; SNAP = sensory nerve action potential.

reduced compound muscle action potential, a conduction block in the tibial nerve and slightly reduced nerve conduction velocities, but no temporal dispersion, fulfilling the electrophysiological diagnostic criteria of acute inflammatory demyelinating polyradiculoneuropathy (Hadden *et al.*, 1998). No spontaneous activity was recordable on EMG at any time. The patient was diagnosed with GBS and treated with five plasma exchanges. Recovery started 4 weeks after onset. The course of disease was monophasic. At a follow-up visit in our department 1 year after the diagnosis of GBS, the patient did not present any neurological deficits or pain. Nerve conduction studies were nearly normal, the conduction block of the tibial nerve was no longer present (Supplementary Fig. 3). A follow-up serum sample was obtained in April 2016 and did not show any binding to murine teased fibres or Caspr-transfected HEK293 cells as assessed by fluorescence microscopy and flow cytometry.

Destruction of paranodal/nodal architecture in the sural nerve biopsy and skin biopsies

Sural nerve biopsy of Patient 1 and skin biopsies of the distal and proximal leg and finger were obtained in 2014 for diagnostic work-up. No sensory nerve action potential was measurable in the sural nerve at this time-point. Sural nerve biopsy revealed subperineurial oedema, severe axonal loss, numerous degenerating axons, but only a few thinly myelinated fibres and no onion bulbs; thus showing features of axonal damage but no features of de- or remyelination (Supplementary Fig. 4). The number of endoneurial T cells was only mildly increased. Skin biopsies revealed a normal intraepidermal nerve fibre density of 12.2 fibres/mm at the distal leg and 16.9 fibres/mm at the proximal leg. Paranodal and nodal architecture was studied using teased fibres of the sural nerve biopsy and skin biopsy sections from the lateral index finger. We found severe dispersion of Caspr and neurofascin staining in teased fibres of the sural nerve and dermal myelinated fibres (Fig. 4A, C and D), similar to the findings in skin biopsies of patients with anti-contactin-1 autoantibodies (Doppler *et al.*, 2015*b*). Numerous elongated nodes of Ranvier were detectable, but dispersion of Caspr and neurofascin staining was also found at nodes of normal length (Fig. 4D). Remarkably, morphological changes were not restricted to paranodal proteins. Immunofluorescence staining with anti-pan-sodium channel revealed lengthening of the band of sodium channels at many nodes (Fig. 4B).

Deposition of human IgG at the paranodes

Immunofluorescence labelling of human IgG was performed on teased fibre preparations of the sural nerve biopsy of

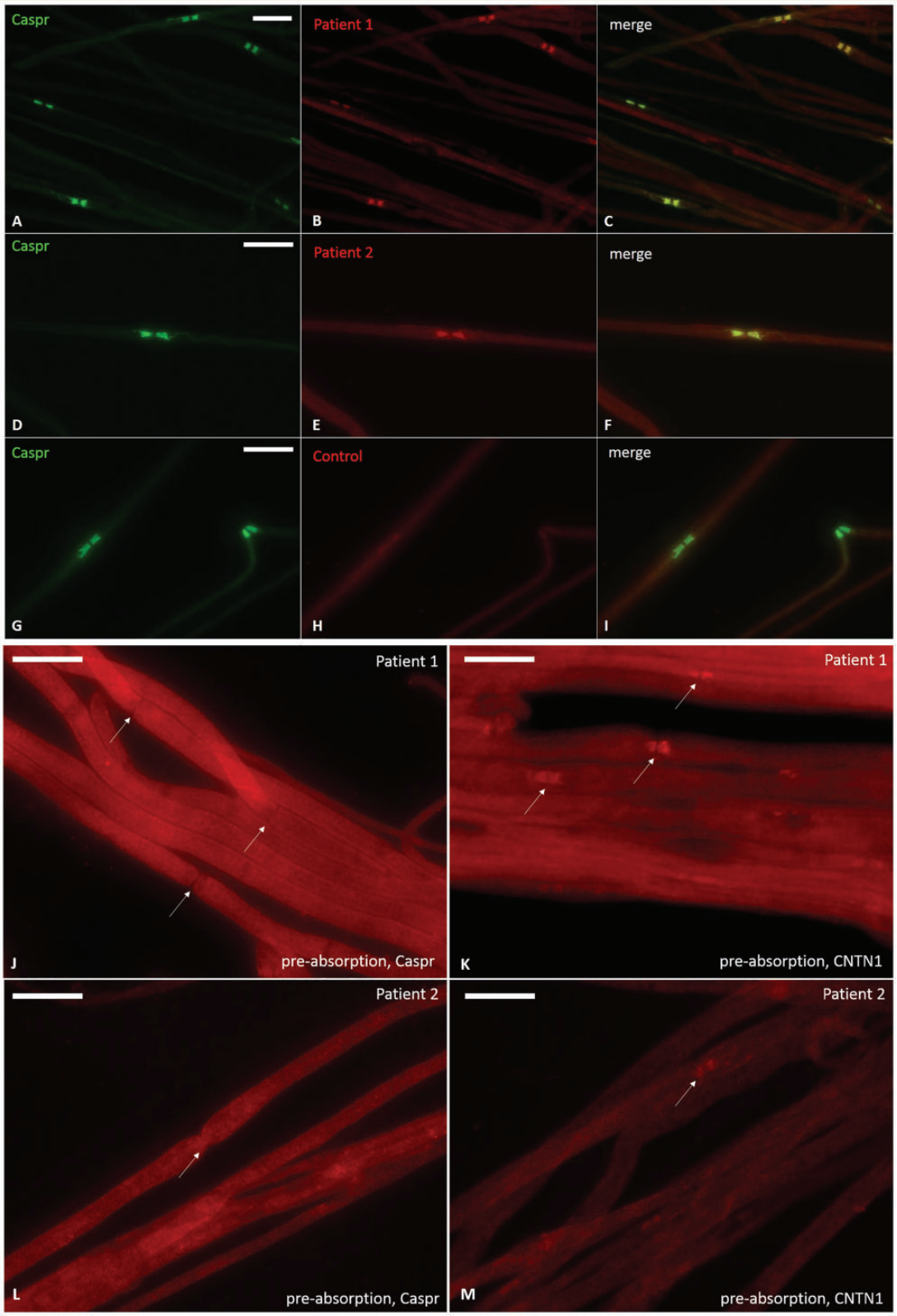

Figure 1 Photomicrograph of binding assays of patients' samples with murine teased fibre stained with anti-Caspr. Patient 1 (**A**–**C**) and 2 (**D**–**F**) show distinct binding to the paranodes (**B** and **E**) co-localizing with the immunoreactivity of anti-Caspr (**A** and **D**). Serum of a normal control does not bind to the paranodes (**G**–**I**). Photomicrographs of murine teased fibres, incubated with patients' samples after preincubation with Caspr- (**J** and **L**) and contactin-1- (**K** and **M**) transfected HEK293 cells. Preincubation with Caspr-transfected HEK293 cells results in loss of paranodal deposition of IgG (**J** and **L**), preincubation with contactin-1-transfected HEK293 cells does not (**K** and **M**).

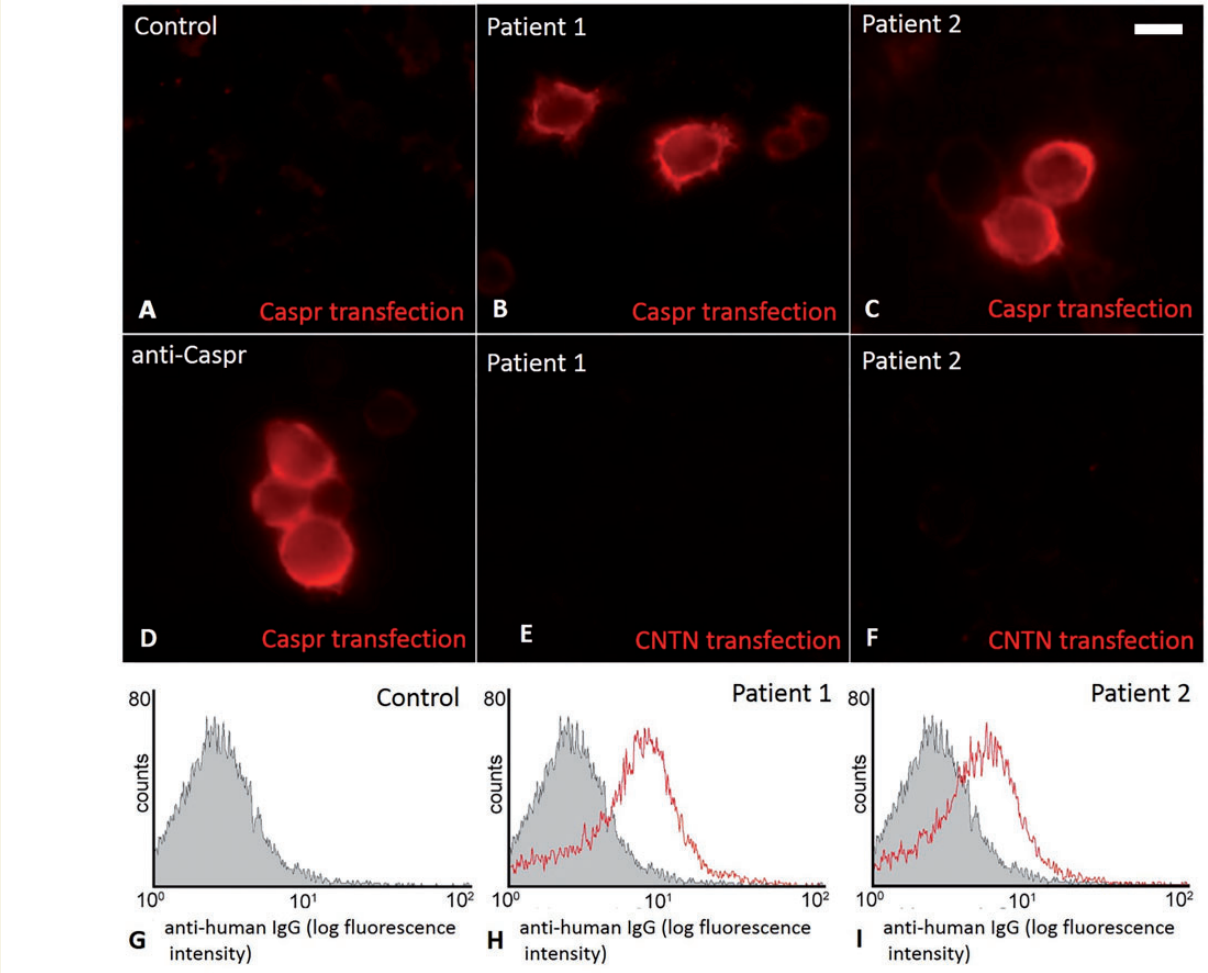

Figure 2 Binding assays of patients' samples with Caspr- and CNTN1-transfected HEK293. Photomicrographs of binding assays of patients' samples with Caspr-transfected HEK293 (**B** and **C**) cells and contactin-1-transfected cells as a control (**E** and **F**). Both patients as well as commercial anti-Caspr show clear binding to Caspr-transfected HEK293 cells (**B**–**D**), but lack of binding to contactin-1 transfected HEK293 cells (**E** and **F**). A normal control does not bind to Caspr-transfected HEK293 cells (**A**). When quantified by flow cytometry, binding is confirmed by higher fluorescence intensity of the binding of patients' sera compared to controls (**G**–**I**). Grey areas indicate the fluorescence of the normal controls, red lines indicate patients' samples.

Patient 1 to demonstrate binding of patient's IgG to the paranodes *in vivo*. Indeed, paranodes were immunoreactive for human IgG in the sural nerve biopsy of Patient 1, but not in a nerve biopsy of a patient with non-inflammatory peripheral neuropathy that served as control (Fig. 5).

Binding to paranodes of motor and sensory nerve fibres and non-paranodal tissue

As motor symptoms were more severe than sensory deficits in both patients, binding to motor nerve fibres (ventral roots) and sensory nerve fibres (dorsal roots) was assessed in comparison. Strong binding to the paranodes of fibres of the ventral root was detected, but only weak binding to the paranodes of dorsal roots (Supplementary Fig. 5).

Binding to neuronal structures such as cerebellum, hippocampal neurons or DRGs has been described in sera with autoantibodies against other paranodal proteins, namely contactin-1 and neurofascin-155 (Querol *et al.*, 2013, 2014; Doppler *et al.*, 2015*b*; Miura *et al.*, 2015). We therefore investigated binding of the samples of our patients with anti-Caspr autoantibodies to cerebellum, spinal cord, cerebrum, hippocampal neurons, motor neurons and DRG (sections and cultured neurons). We did not detect any binding of patients' samples to tissue of the CNS (including spinal cord and motor neurons), but both sera bound to small DRG neurons of DRG sections and cultured DRG (Fig. 6 and Supplementary Fig. 6). Double labelling for TRPV1 and IB4 displayed that these neurons were TRPV1-positive and most of them were also IB4-positive (Fig. 6 and Supplementary Fig. 6). Pre-absorption of sera with Caspr-transfected HEK293 cells prior to the binding

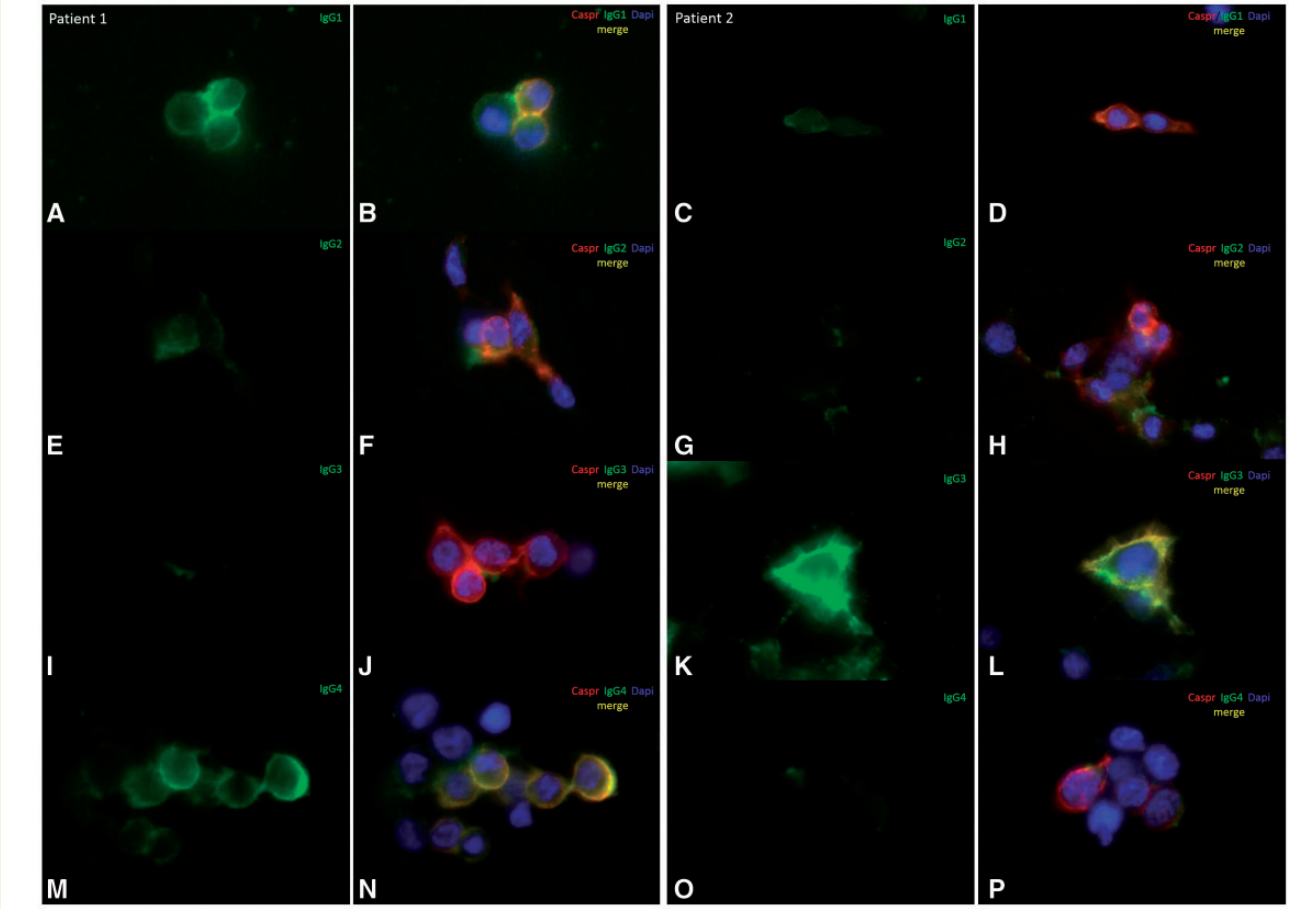

Figure 3 Binding assays of patients' samples with Caspr-transfected HEK293 cells using secondary antibodies against different subclasses of human IgG. Photomicrographs of immunofluorescence binding assays of patients' samples (green), anti-Caspr (red) and DAPI with Caspr-transfected HEK293 cells using secondary antibodies against different subclasses of human IgG. Co-localization is displayed in yellow. Weak binding of anti-IgG1 is detectable in Patient 1 (**A** and **B**), but not in Patient 2 (**C** and **D**). No binding of anti-IgG2 can be found in both patients (**E**–**H**). Strong reactivity of anti-IgG3 is found in Patient 2 (**K** and **L**), not in Patient 1 (**I** and **J**). Anti-IgG4 shows strong immunoreactivity in Patient 1 (**M** and **N**) but is negative in Patient 2 (**O** and **P**).

assays with DRG sections and neurons prevented binding of patients' IgG (Fig. 6 and Supplementary Fig. 7).

Complement binding assay

Complement binding assays with samples of both patients with Caspr-transfected HEK293 cells were performed. Distinct binding of C1q by HEK293 cells after binding of patients' IgG was only found in Patient 2 who mainly had IgG3 anti-Caspr autoantibodies, not in Patient 1, where IgG4 was the predominant subclass (Supplementary Fig. 8).

Discussion

Here, we give the first description of autoantibodies against the paranodal protein Caspr in patients with inflammatory neuropathies and provide a detailed clinical and histopathological description of this condition, including evidence of binding of IgG to the paranodes in a patient's sural nerve. The clinical picture of the patient with anti-Caspr associated CIDP very much resembles the symptoms described in patients with autoantibodies against neurofascin-155 and contactin-1, namely acute onset of severe motor more than sensory neuropathy, very good response to treatment with rituximab, and demyelinating features in nerve conduction studies, in contrast to axonal degeneration in nerve biopsies (Querol *et al.*, 2013, 2014, 2015; Doppler *et al.*, 2015*b*; Miura *et al.*, 2015). However, in comparison to patients with anti-contactin-1 or anti-neurofascin-155 autoantibodies, our patients did not present with cerebellar tremor or spinal ataxia, and sera did not bind to cerebellum, hippocampal neurons or large DRG neurons (Querol *et al.*, 2013; Miura *et al.*, 2015). Instead, we detected binding of both samples to small diameter TRPV1-immunoreactive DRG neurons that are supposed to be involved in pain perception. In both patients, pain was the first symptom and both suffered from severe neuropathic pain requiring treatment with pregabalin or opioids. Neuropathic pain has not been described in patients with

Table 2 Course of disease in Patient 1

Date of assessment	03/2013	04/2014	07/2014	12/2014	01/2015	05/2015	08/2015	02/2016
Treatment	IVIG: ineffective, steroids: slight improvement for some weeks	PE: stabilization (no further progression)	PE, rituximab (first cycle): improvement	PE, steroids (given because of relapse associated with infection)	Rituximab (second cycle)	Rituximab (third cycle)	Rituximab (fourth cycle)	
MRC grade	Tibialis anterior muscle 4, other muscles 5	Upper limbs: proximal 4, distal 0–3, lower limbs: proximal 4, distal 0	Upper limbs: proximal 4, distal 0–4, lower limbs: proximal 4, distal 0	Upper limbs: proximal 5, distal 0–4, lower limbs: proximal 4, distal 0–1	Proximal 5, distal 1–2, proximal 5, distal 0–2	Proximal 5, distal 2–4, proximal 5, distal 1–2	Proximal 5, distal 3–4, proximal 5, distal 1–2	Proximal 5, distal 4, proximal 5, distal 1–2
MRC sum score (Kleyweg *et al.*, 1991)	58/60	44/60	44/60	48/60	52/60	52/60	52/60	54/60
Hypesthesia	Feet and hands	From Th4 downwards and of the hands and lower arms	Feet and hands	Lower arms and legs	None	None	None	None
Pain	Severe	Severe	Severe	Severe	Moderate	Rarely	None	None
Analgesics (mg/day)	None	Amitriptyline 75, tilidine 300	Pregabalin 600, tilidine 600	Pregabalin 600, 450	Pregabalin 75, tilidine 100	Pregabalin 150, tilidine 100	None	None
Ambulation	Crutches, stairs possible	Mostly wheelchair-bound, crutches for shorter distances	Mostly wheelchair-bound, crutches for shorter distances	Crutches, stairs impossible	Crutches, stairs possible	One crutch, stairs possible	Without aid	Without aid
CSF	8 cells/μl, protein 5.2 g/l	46 cells/μl, protein 1.7 g/l	Not done	Not done	Not done	Not done	Not done	Not done
Nerve conduction studies	Right peroneal, left tibial nerve: NCV 35/38 m/s, DML 8.2/7.8 ms, CMAP 3.2 mV/4 mV, CB of the right tibial nerve; right median and ulnar nerve: DML 8.3/8.5 ms, NCV 32.2/33.4 mV, normal CMAP, F-waves 35/34.2 ms, normal SNAP and NCV of the sural and sensory median nerve	Right median nerve: DML 23.8 ms, CMAP 0.12 MV, NCV 12.8 m/s, other nerves not recordable, EMG: many fibrillations and positive sharp waves in distal > proximal muscles	Right median nerve: DML 22.8 ms, CMAP 0.09 mV, NCV 12.4 m/s, other nerves not recordable	Not done	Not done	Right median nerve: DML 9.5 ms, CMAP 0.6 mV, NCV 24 m/s	Not done	Right median nerve: DML 5.7 ms, CMAP 0.4 mV, NCV 19.8 m/s, right tibial nerve: DML 11.7 ms, CMAP 0.1 mV, NCV 22.8 m/s
Binding assays murine teased fibres	Not done	Paranodal binding	Paranodal binding	No binding	No binding	Not done	No binding	Not done
Binding assays HEK cells	Not done	Strong binding to Caspr-transfected cells	Strong binding to Caspr-transfected cells	Weak binding to Caspr-transfected cells	No binding to Caspr-transfected cells	Not done	No binding to Caspr-transfected cells	Not done

CB = conduction block; CMAP = compound muscle action potential; DML = distal motor latency; IVIG = intravenous immunoglobulins; MRC = Medical Research Council; NCV = nerve conduction velocity; PE = plasma exchange; SNAP = sensory nerve action potential.

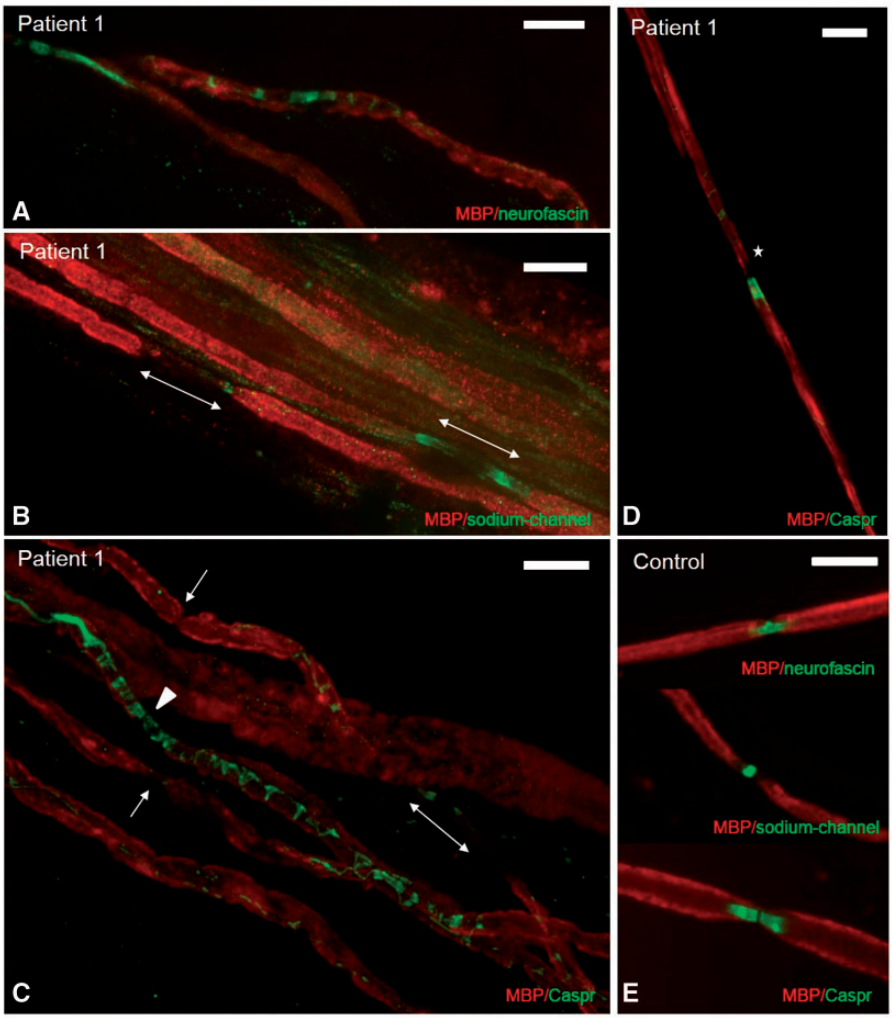

Figure 4 Destruction of nodal architecture in teased fibres of the sural nerve of Patient 1. Photomicrographs of teased fibres of the sural nerve of Patient 1. (**A**–**D**) and a normal control (**E**), double-labelled with anti-MBP (red) and anti-neurofascin/anti-pan-sodium-channel/anti-Caspr (green). Disruption of neurofascin-immunoreactivity (**A**) and of the band of sodium channels (**B**) is detected in Patient 1. Two elongated nodes are detectable (double-ended arrows). Almost complete loss of Caspr-immunoreactivity is found at some nodes (**C**, arrows) or at one side of the node (**D**, asterisks). Dispersion of Caspr to the juxtaparanodes and internodes is detected in another nerve fibre (**C**, arrowheads), as well as an elongated node of Ranvier (**C**, double arrow). Scale bars = 10 μm. See Supplementary material for single channel images of this figure.

autoantibodies against other paranodal proteins so far, but some patients with chronic idiopathic pain have autoantibodies against the juxtaparanodal protein Caspr-2 (Klein *et al.*, 2012). Pain resolved shortly after treatment with rituximab in Patient 1 and resolved completely in Patient 2 after recovery. The quick relief of pain after treatment as well as normal intraepidermal nerve fibre density as detected in Patient 1 argues against small nerve fibre or neuronal damage in these patients but rather for a functional effect by antibody binding to nociceptive neurons. As described in other neuropathies with autoantibodies against paranodal proteins (Querol *et al.*, 2013, 2014; Doppler *et al.*, 2015*b*; Miura *et al.*, 2015), motor symptoms were more severe than sensory deficits in both patients. This might correlate with stronger binding of both sera to the paranodes of motor fibres compared to sensory fibres as observed in our study. Exclusive binding to ventral but not dorsal roots has recently been described in a passive transfer rat model with autoantibodies against contactin-1 (Manso *et al.*, 2016) and was observed in acute motor axonal neuropathy (AMAN) patients with anti-GD1a autoantibodies (De Angelis *et al.*, 2001). However, weak binding to sensory fibres as well as severe destruction of paranodal architecture in the sural nerve in our study reflects sensory involvement, though less dominant than motor symptoms.

So far, autoantibodies against paranodal proteins have been described as associated with CIDP but not with GBS (Querol *et al.*, 2013; Doppler *et al.*, 2015*b*), with the exception of anti-contactin-1 in rare cases of GBS, though without binding to paranodes (Miura *et al.*, 2015). In the present study, we show distinct binding of antibodies of a

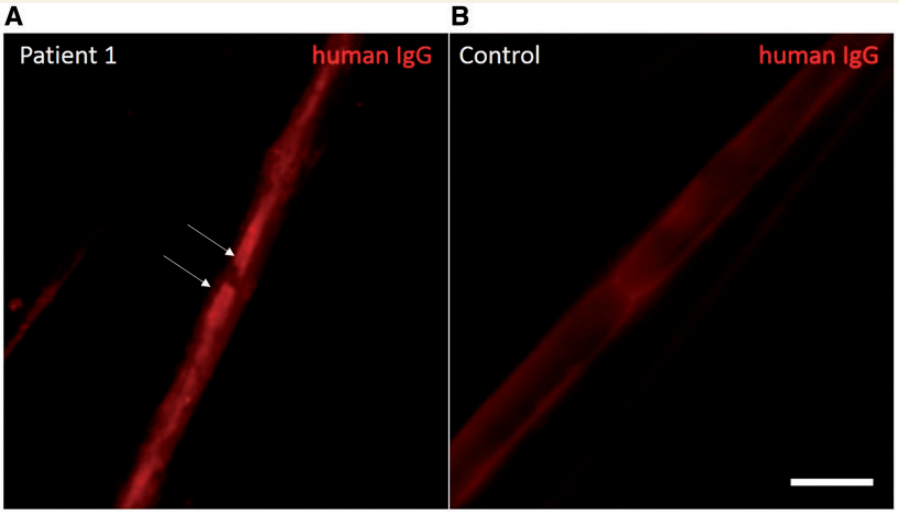

Figure 5 Immunoglobulin deposition at the paranodes of teased fibres of the sural nerve biopsy of Patient 1. Photomicrograph of teased fibres of the sural nerve biopsy of Patient 1. (**A**) and a control with non-inflammatory neuropathy (**B**), incubated with anti-human IgG. Deposition of human IgG at the paranodes (arrows) is detected in Patient 1 (**A**), probably corresponding to the binding of anti-Caspr autoantibodies at the paranodes. No binding is present when using a control nerve (**B**). Scale bar = 10 μm.

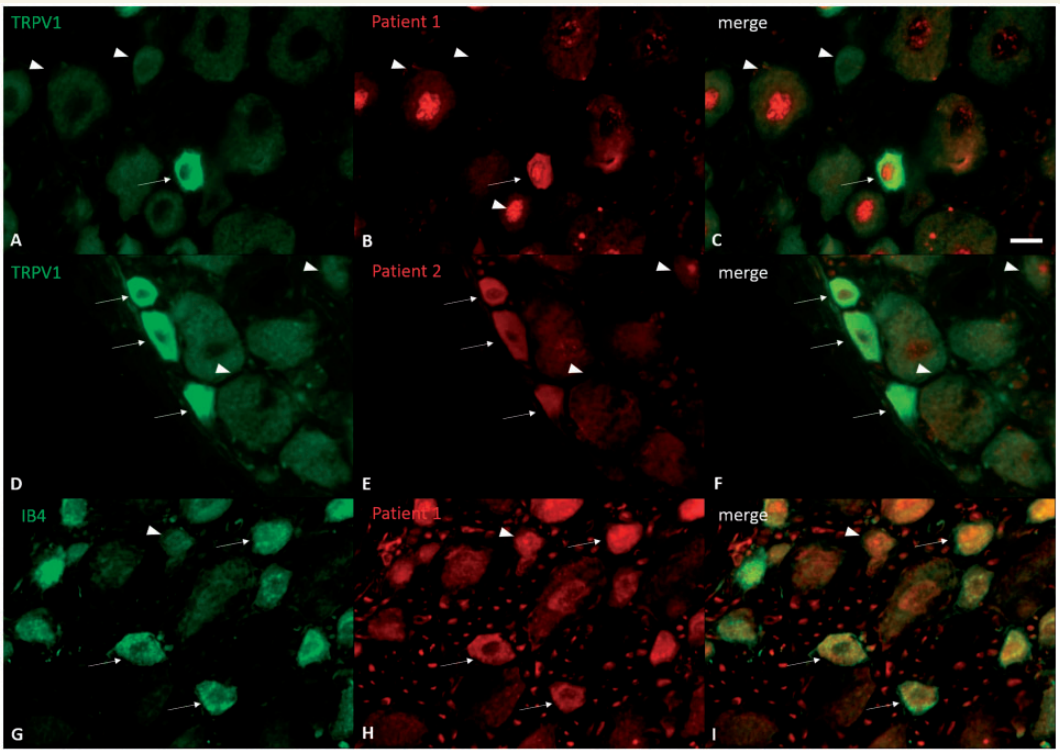

Figure 6 Binding of patients' sera to small DRG neurons. Photomicrograph of a DRG section double stained with patient samples (**B, E** and **H**) and anti-TRPV1 (**A** and **D**) and IB4 (**G**). **C, F** and **I** are overlays. Both patients show binding to TRPV1-positive small neurons (arrows), not to large neurons or TRPV1-negative small neurons (arrowheads). Some of the small neurons that bind patient IgG are also immunoreactive for anti-IB4 (arrows), some are not (arrowheads). Scale bar = 20 mm.

patient with GBS to the paranodes and confirmed anti-Caspr autoantibodies by binding assays with Caspr-transfected HEK293 cells. In contrast to Patient 1, who was diagnosed with CIDP and to the other published patients with autoantibodies against paranodal proteins (Querol *et al.*, 2013, 2014; Doppler *et al.*, 2015*b*), no fibrillations or positive sharp waves were found in Patient 2 by EMG, arguing against axonal damage. This finding may support

the notion that binding of autoantibodies to the paranodes alone can lead to a disruption of nerve conduction, not only by induction of secondary axonal degeneration. A rapid improvement of symptoms as usually seen in GBS seems to be possible if the production of autoantibodies does not persist. This pattern of acute neuropathy with autoantibodies, quick recovery and absence of spontaneous activity or temporal dispersion resembles a condition that was described as a possible variant of AMAN associated with anti-ganglioside autoantibodies: it has been hypothesized that autoantibodies against gangliosides might induce reversible conduction failure at the nodes leading to a variant of AMAN, termed AMAN with reversible conduction block or acute motor conduction block neuropathy, that can go along with quick recovery if no secondary axonal damage occurs (Capasso *et al.*, 2003; Kuwabara and Yuki, 2013). This condition was recently summarized by the term 'nodo-paranodopathy', emphasizing the node of Ranvier as the site of pathogenic attack (Uncini, 2012; Uncini *et al.*, 2013). Histopathological evidence of paranodal disruption in patients with autoantibodies against contactin-1 led to the idea that the term 'paranodopathy' might also be appropriate for the new entity of neuropathies with autoantibodies against paranodal proteins (Doppler *et al.*, 2015*b*). Previously, we could not further strengthen the idea because reversible conduction failure could not be demonstrated in our cohort of patients with anti-contactin-1 autoantibodies due to severe secondary axonal degeneration in all patients (Doppler *et al.*, 2015*b*). The detection of anti-Caspr autoantibodies in a new patient (Patient 2) with the clinical picture of GBS with reversible conduction block supports the idea of the concept of paranodopathy in patients with autoantibodies against paranodal proteins. Remarkably, autoantibodies of the subclass IgG3 were detected in this patient and complement deposition was found. Thus, dysfunction of the nodal/paranodal complex may be complement-mediated in GBS with reversible conduction block and anti-Caspr autoantibodies, similar to what has been assumed in patients with anti-ganglioside autoantibodies (Susuki *et al.*, 2012). Patient 1 also fits into the concept of paranodopathy, but in addition he had secondary axonal degeneration leading to spontaneous activity on EMG. This may explain the long delay of recovery after treatment with rituximab and subsequent decline of anti-Caspr titres.

As already described in patients with anti-contactin-1 autoantibodies (Doppler *et al.*, 2015*b*), the nerve biopsy of the patient with anti-Caspr did not show classical features of demyelination like thinly myelinated fibres or onion bulbs, indicating that the paranodes/nodes of Ranvier are the site of attack in this subtype of inflammatory neuropathy rather than the myelin sheath (Uncini, 2012; Uncini *et al.*, 2013). Indeed, severe disruption of the paranodal region and lengthening of the nodal gap were detectable in teased fibres of the sural nerve of our patient as well as in skin dermal nerve fibres. Furthermore, we could demonstrate dispersion of sodium channels to the paranodes as well as disruption of the band of sodium channels in elongated nodes of Ranvier. This may be the morphological equivalent of impaired nerve conduction at the nodes of Ranvier. It resembles nodal changes that were described in rabbits immunized with gangliosides and in mice lacking gangliosides (Susuki *et al.*, 2007*a, b*) but never in patients with CIDP without the detection of autoantibodies (Li *et al.*, 2005; Doppler *et al.*, 2013).

Destruction of the paranodal architecture indicates a pathogenic effect of autoantibodies affecting the paranodes that is strengthened by the detection of deposition of IgG at the paranodes in the sural nerve of Patient 1. However, the exact pathogenic link between binding of autoantibodies and paranodal destruction in patients with IgG4 autoantibodies remains to be established. We did not detect any binding of complement by complement binding assay in Patient 1, which is consistent with the predominance of IgG4 antibodies that do not bind complement. Functional disturbance of the paranodal adhesion molecules may underlie paranodal destruction and impairment of nerve conduction, as already hypothesized in patients with anti-contactin-1 autoantibodies (Labasque *et al.*, 2014).

The presence of different subclasses of IgG in patients with anti-Caspr autoantibodies, namely IgG3 in the patient with GBS and IgG4 in the patient with CIDP, is consistent with a recent study of patients with anti-contactin-1 autoantibodies. In this former study we also found a predominance of IgG3 in two patients who were tested during the acute GBS-like beginning of CIDP and two with IgG4 who were analysed during the chronic phase of disease (Doppler *et al.*, 2015*b*). The current findings support the idea of a switch to IgG4 at the chronic phase of disease.

Summary

In summary, our study demonstrates that Caspr is another antigen in the subgroup of inflammatory neuropathies with autoantibodies against paranodal proteins and that a monophasic course of disease may occur. In contrast to other neuropathies with antibodies to the paranodal complex (anti-contactin-1, anti-neurofascin-155) both patients with autoantibodies against Caspr suffered from severe neuropathic pain. However, larger studies are needed to clarify if neuropathic pain is a distinct feature of anti-Caspr-associated neuropathy. We give further evidence that 'paranodopathies' with autoantibodies against the paranodal complex represent a well-defined entity within the spectrum of inflammatory neuropathies with excellent response to treatment with rituximab. This entity needs to be taken into account in the diagnostic work-up of patients with peripheral neuropathy as it represents a treatable condition, where treatment significantly differs from the current first-line treatments of CIDP.

Acknowledgements

We thank Nadine Vornberger, Barbara Reuter and Barbara Dekant for excellent technical assistance. We thank E. Meinl and J.K.M. Ng for providing reagents for the neurofascin ELISA.

Funding

The study was supported by research funds of the University of Würzburg. K.D. is supported by a grant ('Habilitationsstipendium') from the Faculty of Medicine, University of Würzburg. L.A. is supported by a grant of the Graduate School of Life Sciences of the University of Würzburg. C.M. is supported by a grant from the IZKF (interdisciplinary center for clinical research) Würzburg. C.S. and C.V. are funded by Deutsche Forschungsgemeinschaft, SO 328/9-1 and VI 586/7-1.

Supplementary material

Supplementary material is available at *Brain* online.

References

Capasso M, Caporale CM, Pomilio F, Gandolfi P, Lugaresi A, Uncini A. Acute motor conduction block neuropathy Another Guillain-Barre syndrome variant. Neurology 2003; 61: 617–22.

De Angelis MV, Di Muzio A, Lupo S, Gambi D, Uncini A, Lugaresi A. Anti-GD1a antibodies from an acute motor axonal neuropathy patient selectively bind to motor nerve fiber nodes of Ranvier. J Neuroimmunol 2001; 121: 79–82.

Devaux JJ, Odaka M, Yuki N. Nodal proteins are target antigens in Guillain-Barre syndrome. J Peripher Nerv Syst 2012; 17: 62–71.

Dib-Hajj SD, Choi JS, Macala LJ, Tyrrell L, Black JA, Cummins TR, et al. Transfection of rat or mouse neurons by biolistics or electroporation. Nat Protoc 2009; 4: 1118–26.

Doppler K, Appeltshauser L, Kramer HH, Ng JK, Meinl E, Villmann C, et al. Contactin-1 and Neurofascin-155/-186 Are Not Targets of Auto-Antibodies in Multifocal Motor Neuropathy. PLoS One 2015a; 10: e0134274.

Doppler K, Appeltshauser L, Wilhelmi K, Villmann C, Dib-Hajj SD, Waxman SG, et al. Destruction of paranodal architecture in inflammatory neuropathy with anti-contactin-1 autoantibodies. J Neurol Neurosurg Psychiatry 2015b; 86: 720–8.

Doppler K, Werner C, Sommer C. Disruption of nodal architecture in skin biopsies of patients with demyelinating neuropathies. J Peripher Nerv Syst 2013; 18: 168–76.

Dupree JL, Girault JA, Popko B. Axo-glial interactions regulate the localization of axonal paranodal proteins. J Cell Biol 1999; 147: 1145–52.

Dyck PJ, Dyck PJB, Engelstad J. Pathological alterations of nerves. In: Peripheral neuropathy. Philadelphia, PA: Elsevier Saunders; 2005. p. 733–829.

Faivre-Sarrailh C, Gauthier F, Denisenko-Nehrbass N, Le Bivic A, Rougon G, Girault JA. The glycosylphosphatidyl inositol-anchored adhesion molecule F3/contactin is required for surface transport of paranodin/contactin-associated protein (caspr). J Cell Biol 2000; 149: 491–502.

Hadden RD, Cornblath DR, Hughes RA, Zielasek J, Hartung HP, Toyka KV, et al. Electrophysiological classification of Guillain-Barre syndrome: clinical associations and outcome. Plasma Exchange/Sandoglobulin Guillain-Barre Syndrome Trial Group. Ann Neurol 1998; 44: 780–8.

Hughes RA, Donofrio P, Bril V, Dalakas MC, Deng C, Hanna K, et al. Intravenous immune globulin (10% caprylate-chromatography purified) for the treatment of chronic inflammatory demyelinating polyradiculoneuropathy (ICE study): a randomised placebo-controlled trial. Lancet Neurol 2008; 7: 136–44.

Klein CJ, Lennon VA, Aston PA, McKeon A, Pittock SJ. Chronic pain as a manifestation of potassium channel-complex autoimmunity. Neurology 2012; 79: 1136–44.

Kleyweg RP, van der Meche FG, Schmitz PI. Interobserver agreement in the assessment of muscle strength and functional abilities in Guillain-Barre syndrome. Muscle Nerve 1991; 14: 1103–9.

Kuwabara S, Yuki N. Axonal Guillain-Barre syndrome: concepts and controversies. Lancet Neurol 2013; 12: 1180–8.

Labasque M, Hivert B, Nogales-Gadea G, Querol L, Illa I, Faivre-Sarrailh C. Specific contactin N-glycans are implicated in neurofascin binding and autoimmune targeting in peripheral neuropathies. J Biol Chem 2014; 289: 7907–18.

Lauria G, Hsieh ST, Johansson O, Kennedy WR, Leger JM, Mellgren SI, et al. European Federation of Neurological Societies/Peripheral Nerve Society Guideline on the use of skin biopsy in the diagnosis of small fiber neuropathy. Report of a joint task force of the European Federation of Neurological Societies and the Peripheral Nerve Society. Eur J Neurol 2010; 17: 903–12, e44-9.

Li J, Bai Y, Ghandour K, Qin P, Grandis M, Trostinskaia A, et al. Skin biopsies in myelin-related neuropathies: bringing molecular pathology to the bedside. Brain 2005; 128: 1168–77.

Manso C, Querol L, Mekaouche M, Illa I, Devaux JJ. Contactin-1 IgG4 antibodies cause paranode dismantling and conduction defects. Brain 2016; 139 (Pt 6): 1700–12.

Miura Y, Devaux JJ, Fukami Y, Manso C, Belghazi M, Wong AH, et al. Contactin 1 IgG4 associates to chronic inflammatory demyelinating polyneuropathy with sensory ataxia. Brain 2015; 138 (Pt 6): 1484–91.

Ng JK, Malotka J, Kawakami N, Derfuss T, Khademi M, Olsson T, et al. Neurofascin as a target for autoantibodies in peripheral neuropathies. Neurology 2012; 79: 2241–8.

Peles E, Nativ M, Campbell PL, Sakurai T, Martinez R, Lev S, et al. The carbonic anhydrase domain of receptor tyrosine phosphatase beta is a functional ligand for the axonal cell recognition molecule contactin. Cell 1995; 82: 251–60.

Peles E, Nativ M, Lustig M, Grumet M, Schilling J, Martinez R, et al. Identification of a novel contactin-associated transmembrane receptor with multiple domains implicated in protein-protein interactions. Embo J 1997; 16: 978–88.

Querol L, Nogales-Gadea G, Rojas-Garcia R, Diaz-Manera J, Pardo J, Ortega-Moreno A, et al. Neurofascin IgG4 antibodies in CIDP associate with disabling tremor and poor response to IVIg. Neurology 2014; 82: 879–86.

Querol L, Nogales-Gadea G, Rojas-Garcia R, Martinez-Hernandez E, Diaz-Manera J, Suarez-Calvet X, et al. Antibodies to contactin-1 in chronic inflammatory demyelinating polyneuropathy. Ann Neurol 2013; 73: 370–80.

Querol L, Rojas-Garcia R, Diaz-Manera J, Barcena J, Pardo J, Ortega-Moreno A, et al. Rituximab in treatment-resistant CIDP with antibodies against paranodal proteins. Neurol Neuroimmunol Neuroinflamm 2015; 2: e149.

Sejvar JJ, Kohl KS, Gidudu J, Amato A, Bakshi N, Baxter R, et al. Guillain-Barre syndrome and Fisher syndrome: case definitions and guidelines for collection, analysis, and presentation of immunization safety data. Vaccine 2011; 29: 599–612.

Susuki K, Baba H, Tohyama K, Kanai K, Kuwabara S, Hirata K, et al. Gangliosides contribute to stability of paranodal junctions and ion channel clusters in myelinated nerve fibers. Glia 2007a; 55: 746–57.

Susuki K, Rasband MN. Molecular mechanisms of node of Ranvier formation. Curr Opin Cell Biol 2008; 20: 616–23.

Susuki K, Rasband MN, Tohyama K, Koibuchi K, Okamoto S, Funakoshi K, et al. Anti-GM1 antibodies cause complement-mediated disruption of sodium channel clusters in peripheral motor nerve fibers. J Neurosci 2007b; 27: 3956–67.

Susuki K, Yuki N, Schafer DP, Hirata K, Zhang G, Funakoshi K, et al. Dysfunction of nodes of Ranvier: a mechanism for anti-ganglioside antibody-mediated neuropathies. Exp Neurol 2012; 233: 534–42.

Uncini A. A common mechanism and a new categorization for anti-ganglioside antibody-mediated neuropathies. Exp Neurol 2012; 235: 513–16.

Uncini A, Susuki K, Yuki N. Nodo-paranodopathy: beyond the demyelinating and axonal classification in anti-ganglioside antibody-mediated neuropathies. Clin Neurophysiol 2013; 124: 1928–34.